Practical guide to the realization of a convertible optical trapping system

CHENGLONG ZHAO[1,2,*]

[1]*Department of Electro-Optics and Photonics, University of Dayton, 300 College Park, Dayton, OH 45469, USA*
[2]*Department of Physics, University of Dayton, 300 College Park, Dayton, OH 45469, USA*
*czhao1@udayton.edu

Abstract: In this article, we provide a detailed guide to the construction of a convertible optical trapping system for either single-beam or counter-propagating trap. The single-beam trap maintains all the functionalities that a conventional optical tweezer has. While the counter-propagating trap allows for the trapping of particles that single-beam trap cannot handle. The counter-propagating trap can be easily switched to a single-beam trap, and vice versa. Therefore, this convertible optical trapping system allows for the trapping and manipulation of particles with a wide variety of sizes and materials.

References and links

1. A. Ashkin, "Acceleration and trapping of particles by radiation pressure," Phys. Rev. Lett. **24**(4), 156–159 (1970).
2. A. Ashkin, J. M. Dziedzic, J. E. Bjorkholm, and S. Chu, "Observation of a single-beam gradient force optical trap for dielectric particles," Opt. Lett. **11**(5), 288–290 (1986).
3. A. Lehmuskero, P. Johansson, H. Rubinsztein-Dunlop, L. Tong, and M. Käll, "Laser trapping of colloidal metal nanoparticles," ACS Nano **9**(4), 3453–3469 (2015).
4. K. Scot C, "Opticla tweezer: a practical guide," JMSA **1**, 64–74 (1995).
5. O. M. Maragò, P. H. Jones, P. G. Gucciardi, G. Volpe, and A. C. Ferrari, "Optical trapping and manipulation of nanostructures," Nat. Nanotechnol. **8**(11), 807–819 (2013).
6. E. A. Coronado, E. R. Encina, and F. D. Stefani, "Optical properties of metallic nanoparticles: manipulating light, heat and forces at the nanoscale," Nanoscale **3**(10), 4042–4059 (2011).
7. P. M. Bendix, L. Jauffred, K. Norregaard, and L. B. Oddershede, "Optical trapping of nanoparticles and quantum Dots," IEEE J. Sel. Top. Quantum Electron. **20**(3), 1–12 (2014).
8. Y. Harada and T. Asakura, "Radiation forces on a dielectric sphere in the Rayleigh scattering regime," Opt. Commun. **124**(5–6), 529–541 (1996).
9. W. M. Lee, P. J. Reece, R. F. Marchington, N. K. Metzger, and K. Dholakia, "Construction and calibration of an optical trap on a fluorescence optical microscope," Nat. Protoc. **2**(12), 3226–3238 (2007).
10. G. Pesce, G. Volpe, O. M. Maragó, P. H. Jones, S. Gigan, A. Sasso, and G. Volpe, "Step-by-step guide to the realization of advanced optical tweezers," J. Opt. Soc. Am. B **32**(5), B84–B98 (2015).
11. K. C. Neuman and S. M. Block, "Optical trapping," Rev. Sci. Instrum. **75**(9), 2787–2809 (2004).
12. A. Gennerich, *Optical Tweezers: Methods and Protocols* (Springer, 2017).
13. A. Ashkin, *Optical Trapping and Manipulation of Neutral Particles Using Lasers: A Reprint Volume with Commentaries* (Word Scientific, 2006).
14. S. E. S. Spesyvtseva and K. Dholakia, "Trapping in a material world," ACS Photonics **3**(5), 719–736 (2016).
15. A. van der Horst, P. D. J. van Oostrum, A. Moroz, A. van Blaaderen, and M. Dogterom, "High trapping forces for high-refractive index particles trapped in dynamic arrays of counterpropagating optical tweezers," Appl. Opt. **47**(17), 3196–3202 (2008).
16. A. Jannasch, A. F. Demirörs, P. D. J. van Oostrum, A. van Blaaderen, and E. Schäffer, "Nanonewton optical force trap employing anti-reflection coated, high-refractive-index titania microspheres," Nat. Photonics **6**(7), 469–473 (2012).
17. Y. Hu, T. A. Nieminen, N. R. Heckenberg, and H. Rubinsztein-Dunlop, "Antireflection coating for improved optical trapping," J. Appl. Phys. **103**(9), 93119 (2008).
18. A. Kyrsting, P. M. Bendix, and L. B. Oddershede, "Mapping 3D focal intensity exposes the stable trapping positions of single nanoparticles," Nano Lett. **13**(1), 31–35 (2013).
19. P. M. Hansen, V. K. Bhatia, N. Harrit, and L. Oddershede, "Expanding the optical trapping range of gold nanoparticles," Nano Lett. **5**(10), 1937–1942 (2005).
20. L. Bosanac, T. Aabo, P. M. Bendix, and L. B. Oddershede, "Efficient optical trapping and visualization of silver

nanoparticles," Nano Lett. **8**(5), 1486–1491 (2008).
21. F. Hajizadeh and S. N. S. Reihani, "Optimized optical trapping of gold nanoparticles," Opt. Express **18**(2), 551–559 (2010).
22. M. Dienerowitz, "Optical manipulation of nanoparticles: a review," J. Nanophotonics **2**(1), 21875 (2008).
23. Y. Seol, A. E. Carpenter, and T. T. Perkins, "Gold nanoparticles: enhanced optical trapping and sensitivity coupled with significant heating," Opt. Lett. **31**(16), 2429–2431 (2006).
24. K. Pearce, F. Wang, and P. J. Reece, "Dark-field optical tweezers for nanometrology of metallic nanoparticles," Opt. Express **19**(25), 25559–25569 (2011).
25. A. Balijepalli, J. J. Gorman, S. K. Gupta, and T. W. LeBrun, "Significantly improved trapping lifetime of nanoparticles in an optical trap using feedback control," Nano Lett. **12**(5), 2347–2351 (2012).
26. A. van der Horst, A. I. Campbell, L. K. van Vugt, D. A. Vanmaekelbergh, M. Dogterom, and A. van Blaaderen, "Manipulating metal-oxide nanowires using counter-propagating optical line tweezers," Opt. Express **15**(18), 11629–11639 (2007).
27. D. L. J. Vossen, A. Van Der Horst, M. Dogterom, and A. Van Blaaderen, "Optical tweezers and confocal microscopy for simultaneous three-dimensional manipulation and imaging in concentrated colloidal dispersions," Rev. Sci. Instrum. **75**(9), 2960–2970 (2004).
28. T. Cizmar, V. Garces-Chavez, K. Dholakia, and P. Zemanek, "Optical trapping in counter-propagating Bessel beams," Proc. SPIE **5514**, 643–651 (2004).
29. S. Tauro, A. Bañas, D. Palima, and J. Glückstad, "Dynamic axial stabilization of counter-propagating beam-traps with feedback control," Opt. Express **18**(17), 18217–18222 (2010).
30. P. Zemánek, A. Jonás, L. Srámek, and M. Liska, "Optical trapping of nanoparticles and microparticles by a Gaussian standing wave," Opt. Lett. **24**(21), 1448–1450 (1999).
31. T. A. Nieminen, V. L. Y. Loke, A. B. Stilgoe, G. Knöner, A. M. Brańczyk, N. R. Heckenberg, and H. Rubinsztein-Dunlop, "Optical tweezers computational toolbox," J. Opt. A, Pure Appl. Opt. **9**(8), S196–S203 (2007).
32. T. A. Nieminen, V. L. Y. Loke, A. B. Stilgoe, N. R. Heckenberg, and H. Rubinsztein-Dunlop, "T-matrix method for modelling optical tweezers," J. Mod. Opt. **58**(5–6), 528–544 (2011).
33. C. J. Murphy, L. B. Thompson, A. M. Alkilany, P. N. Sisco, S. P. Boulos, S. T. Sivapalan, J. A. Yang, D. J. Chernak, and J. Huang, "The many faces of gold nanorods," J. Phys. Chem. Lett. **1**(19), 2867–2875 (2010).
34. P. K. Jain, X. Huang, I. H. El-Sayed, and M. A. El-Sayed, "Noble metals on the nanoscale: optical and photothermal properties and some applications in imaging, sensing, biology, and medicine," Acc. Chem. Res. **41**(12), 1578–1586 (2008).
35. S. Eustis and M. A. el-Sayed, "Why gold nanoparticles are more precious than pretty gold: noble metal surface plasmon resonance and its enhancement of the radiative and nonradiative properties of nanocrystals of different shapes," Chem. Soc. Rev. **35**(3), 209–217 (2006).
36. P. B. Johnson and R. W. Christy, "Optical constants of the noble metals," Phys. Rev. B **6**(12), 4370–4379 (1972).
37. R. Saija, P. Denti, F. Borghese, O. M. Maragò, and M. A. Iatì, "Optical trapping calculations for metal nanoparticles. Comparison with experimental data for Au and Ag spheres," Opt. Express **17**(12), 10231–10241 (2009).
38. K. Svoboda and S. M. Block, "Optical trapping of metallic Rayleigh particles," Opt. Lett. **19**(13), 930–932 (1994).
39. I. M. Peters, B. G. de Grooth, J. M. Schins, C. G. Figdor, and J. Greve, "Three dimensional single-particle tracking with nanometer resolution," Rev. Sci. Instrum. **69**(7), 2762–2766 (1998).
40. A. Pralle, M. Prummer, E. L. Florin, E. H. Stelzer, and J. K. Hörber, "Three-dimensional high-resolution particle tracking for optical tweezers by forward scattered light," Microsc. Res. Tech. **44**(5), 378–386 (1999).
41. A. Rohrbach, H. Kress, and E. H. K. Stelzer, "Three-dimensional tracking of small spheres in focused laser beams: influence of the detection angular aperture," Opt. Lett. **28**(6), 411–413 (2003).
42. F. Gittes and C. F. Schmidt, "Interference model for back-focal-plane displacement detection in optical tweezers," Opt. Lett. **23**(1), 7–9 (1998).
43. A. Rohrbach and E. H. K. Stelzer, "Three-dimensional position detection of optically trapped dielectric particles," J. Appl. Phys. **91**(8), 5474–5488 (2002).
44. J. K. Dreyer, K. Berg-Sørensen, and L. Oddershede, "Improved axial position detection in optical tweezers measurements," Appl. Opt. **43**(10), 1991–1995 (2004).
45. C. Deufel and M. D. Wang, "Detection of forces and displacements along the axial direction in an optical trap," Biophys. J. **90**(2), 657–667 (2006).
46. S. N. S. Reihani and L. B. Oddershede, "Optimizing immersion media refractive index improves optical trapping by compensating spherical aberrations," Opt. Lett. **32**(14), 1998–2000 (2007).
47. D. C. Appleyard, K. Y. Vandermeulen, H. Lee, and M. J. Lang, "Optical trapping for undergraduates," Am. J. Phys. **75**(1), 5–14 (2007).
48. P. M. Hansen, I. M. Tolic-Nørrelykke, H. Flyvbjerg, and K. Berg-Sørensen, "tweezercalib 2.1: Faster version of MatLab package for precise calibration of optical tweezers," Comput. Phys. Commun. **175**(8), 572–573 (2006).
49. O. Brzobohatý, M. Šiler, J. Trojek, L. Chvátal, V. Karásek, A. Paták, Z. Pokorná, F. Mika, and P. Zemánek, "Three-dimensional optical trapping of a plasmonic nanoparticle using low numerical aperture optical tweezers," Sci. Rep. **5**, 8106 (2015).

50. O. Brzobohatý, M. Šiler, J. Trojek, L. Chvátal, V. Karásek, and P. Zemánek, "Non-spherical gold nanoparticles trapped in optical tweezers: shape matters," Opt. Express **23**(7), 8179–8189 (2015).
51. A. Samadi and N. S. Reihani, "Optimal beam diameter for optical tweezers," Opt. Lett. **35**(10), 1494–1496 (2010).
52. M. Mahamdeh, C. P. Campos, and E. Schäffer, "Under-filling trapping objectives optimizes the use of the available laser power in optical tweezers," Opt. Express **19**(12), 11759–11768 (2011).

1. Introduction

Following the seminal work by Ashkin [1,2], optical trapping, which allows for the manipulation of small particles with light, has undergone a rapid development. This technology has become a unique and indispensable tool for both fundamental and applied research in physics, chemistry, biomedicine, and material science. The optical trapping can be realized by either near-field or far-field light. Near-field light allows for the trapping beyond the diffraction limit with reduced laser power. However, trapping with far-field light is preferred in the application where non-invasive manipulation is desired.

A typical far-field optical trapping system traps particles with a single laser beam – optical tweezer or single-beam trap [3–7]. The laser beam is tightly focused on the particle by an objective lens with a high numerical-aperture (NA) so that a strong optical force is generated on the particle. The optical force includes an attractive gradient force and a repelling scattering force. Although this argument is accurate for Rayleigh particles with sizes far smaller than the wavelength of the light, it can be used to understand qualitatively the trapping mechanism [8]. The gradient force originates from the intensity gradient of the focused laser beam and tends to attract the particle to the center of the beam. In contrast, the scattering force, which comes from the radiation pressure of the laser beam, tends to destabilize the trap by pushing the particle towards the laser propagating direction. The gradient force must be large enough to overcome the detrimental scattering force so that a stable trap can be formed, a condition that can be realized by focusing laser beam with a high-NA objective lens. Micro-sized dielectric particles have been successfully trapped with piconewton forces. A step-by-step guide to build a single-beam optical trapping system can be found in [9,10]. The readers are also encouraged to learn more about this technology in [11–13].

Although the trapping of micro-sized dielectric particles has been extensively studied in the past decades, there is an increasing interest to extend the trapping regime to other materials [14] such as high refractive index particles [15], antireflection coated particles [16,17], or metallic nanoparticles [18–25]. The gradient force on these particles is significantly enhanced compared to the force on their dielectric counterparts, but so does the scattering force. Actually, the scattering force can overtake the gradient force in some cases as will be described below. This makes it impossible to trap these particles with single-beam trap. This problem can be solved by applying counter-propagating beams where the scattering forces from each side of the beam counter-acts each other [15,26–30]. However, most counter-propagating traps apply two low-NA objective lenses. This configuration has the following limitations: (1) the weakly focused beams from these lenses generate insufficient optical force to trap particles at the nanoscales; (2) the low-NA objective lenses lack the resolution power to image particles at the nanoscales, while imaging is as important as trapping in these experiments; (3) it lacks the flexibility to switch between single-beam and counter-propagating trap.

In this paper, we give a practical guide to the realization of a convertible optical trapping system that can work compatibly in two modes: single-beam trap or counter-propagating trap. The two working modes can be switched easily, which allows for the trapping of particles with a wide variety of sizes and materials. This article is organized as follows: Section 2 compares the performance of single-beam and counter-propagating trap; Section 3 gives the layout of the convertible trapping system and some considerations for this system; Section 4 gives the details on the realization of the convertible optical trapping system; Finally, Section

5 demonstrates the trapping of both dielectric and highly scattering gold nanoparticles (GNP) on this system.

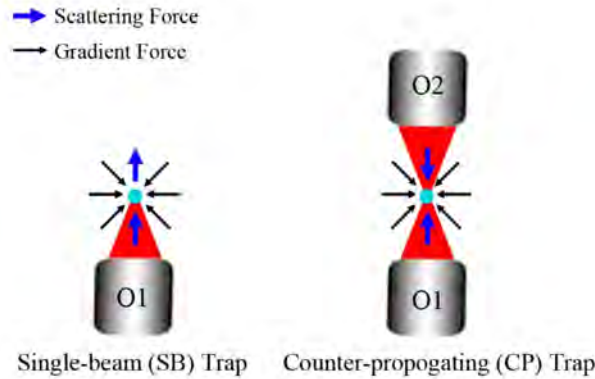## 2. Single-beam (SB) trap vs Counter-propagating (CP) trap

Fig. 1. Compare single-beam and counter-propagating trap.

Figure 1 schematically shows the configuration of a SB trap and a CP trap. In the SB trap, a laser beam is tightly focused by a high-NA objective lens (O1). A nanoparticle at the focus of O1 experiences a gradient force and a scattering force as marked by the black and blue arrows in Fig. 1, respectively. It should be noted that this statement is accurate only if the size of the nanoparticle is much smaller than the laser wavelength [8]. But we can still use this picture to understand qualitatively the trapping mechanism [19]. For highly scattering nanoparticle, such as metallic nanoparticle, the scattering force dominates and pushes the particle out of the trap towards the laser propagating direction. This makes it difficult to trap these nanoparticles with single beam. To overcome this problem, a second beam propagating in the opposite direction can be focused by a second objective lens (O2) to counter-balance the scattering force that comes from O1. The CP trap cancels the detrimental scattering forces along the laser propagating direction, therefore, it allows for the stable trap of highly scattering particles with all sizes and materials.

To get more insight on the trapping difference between the SB and CP trap, we calculated the optical force on gold nanoparticles (GNPs) with the T-matrix method [31,32]. GNPs are chosen not only because they are highly scattering but also because of their intriguing properties [33–35]. In the calculation for SB trap, a laser with a wavelength of 1064 nm is focused in water with an equivalent NA = 1.2. In the calculation for CP trap, two identical beams are focused to the same point in opposite directions. The refractive index of water is taken as $n = 1.33$ and the refractive index of the gold is taken from [36].

Figure 2(a) shows the calculated optical force F_z on a 100 nm (diameter) GNP along the laser propagating direction (z direction) for SB (black curve) and CP (red curve) trap as a function of the particle position. Since the particle escapes mainly along the z direction because of the scattering force, only the optical force in this direction is calculated. The trap strength is determined by the maximum negative restoring force F_{zmax} as marked with a black arrow in Fig. 2(a). In principle, F_{zmax} should be larger than the force of thermal fluctuation to form a stable trap. For the sake of simplicity, we determine whether a GNP is trapped or not based on the sign of the F_{zmax} without taking the thermal fluctuation into account.

For example, there is always a restoring force to pull the particle back to the trapping center if $F_{zmax} < 0$. If $F_{zmax} \geq 0$, the direction of F_z is always towards the laser propagating direction and there is no restoring force to pull the particle back. Therefore, we take $F_{zmax} \geq 0$ as a no- trapping condition. Based on this criteria, it is obvious that the 100 nm GNP can be trapped both in SB and CP trap. However, the trapping center (where $F_z = 0$) in SB trap is

230 nm above the beam center (where z = 0) due to the scattering force. In contrast, the trapping center in a CP trap overlaps with the beam center because of the cancellation of the scattering forces. Figure 2(b) shows the optical force F_z of a 200 nm GNP in SB (black curve) and CP (red curve) trap, respectively. The 200 nm GNP cannot be trapped in SB trap. In contrast, it can be well trapped in the CP trap.
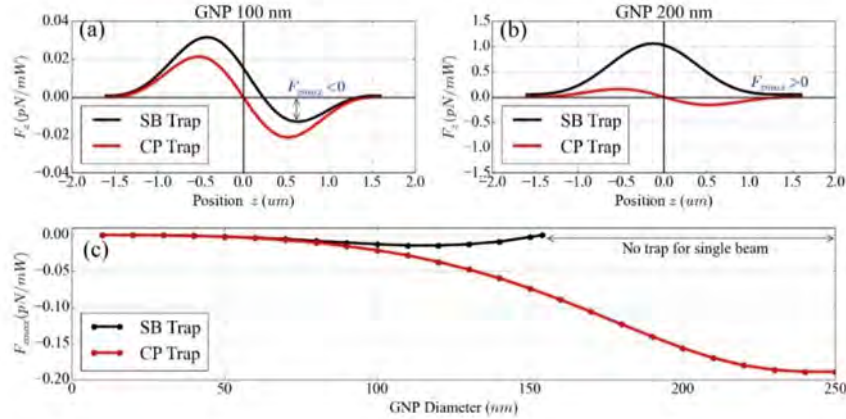

Fig. 2. (a) Calculated optical force along laser propagating direction (z direction) for a 100 nm GNP in single-beam (black solid line) and counter-propagating trap (red solid line). F_{zmax} is the maximum negative restoring force along z direction as marked by the black arrow. (b) The same calculated optical force for a 200 nm GNP in single-beam and counter-propagating trap. (c) Trapping diagram for GNPs with diameters ranging from 10 to 250 nm. SB and CP trap stands for single-beam and counter-propagating trap, respectively.

Figure 2(c) shows the optical force F_{zmax} as a function of particle size ranging from 10 nm to 250 nm (particles with the size in this range are commercially available). The double-sided black arrow indicates that the GNPs cannot be trapped if their sizes fall into this range. For example, the GNP with size larger than 154 nm in diameter cannot be trapped in SB trap. The result agrees with the calculation from [37]. In contrast, GNPs of all sizes can be trapped in
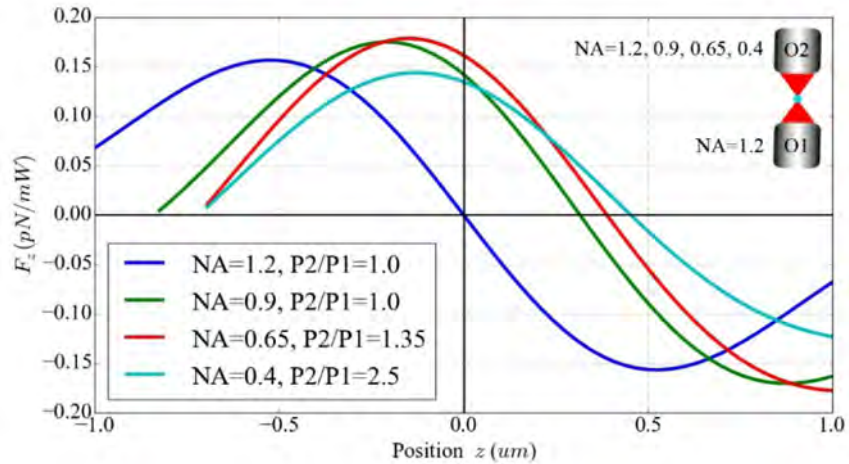

Fig. 3. Calculated optical force along laser propagating direction (z direction) for a 200 nm GNP in CP trap. The NA of the lower objective lens O1 is NA = 1.2, the NA of the upper objective lens O2 changes from NA = 1.2 to NA = 0.4. P2/P1 is the power ratio between the upper and the lower beam.

CP trap. For GNPs smaller than 80 nm, CP trap takes no obvious advantage on SB trap due to the significantly reduced scattering force on smaller particles [38].

The NA of the second objective lens (O2) can be the same or smaller than that of the first one (O1). For example, the NA of O1 in SB trap is typically larger than one (oil or water immersion), which results in a short working distance between the sample and the objective lens. Therefore, O2 with a smaller NA can be chosen to get a larger working space between the sample and the lens. Figure 3 shows the optical force on a 200 nm GNP in a CP trap with different configurations of the two objective lenses. The lower objective lens O1 has a fixed NA = 1.2, the NA of the upper objective lens O2 changes from NA = 1.2 to NA = 0.4. The 200 nm GNP can be well trapped in these four configurations. When the two CP beams with the same laser powers are focused by two identical objective lenses, the trapping position (F_z = 0) overlaps with the beam center (z = 0). When the NA of the O2 is changed to NA = 0.9, the trapping position moved 300 nm above the beam center because of the reduced optical force from O2. The trapping position is 370 nm and 440 nm above the beam center when NA = 0.65 and 0.4, respectively. In order to maintain symmetric optical forces to the trapping position, the power ratio between the two beams needs to be adjusted to P2/P1 = 1.35 and 2.5, respectively. The trapping position in a CP trap can be changed by either adjusting the relative laser powers or the foci of the two beams. This provides a flexible way to tune the position of the trapped particle along the optical axis, which is difficult to achieve in a SB trap.

3. Layout of the convertible optical trapping system

The optical trapping system can be either built directly on a commercial microscope or from scratch. Building the system directly on a microscope is time-saving and mechanically stable, but at the cost of reduced flexibility. In contrast, building the system from scratch requires advanced optical knowledge and skills, but the system is flexible to add custom functions. In this section, a detailed guide to the realization of a home-build convertible optical trapping system is given.
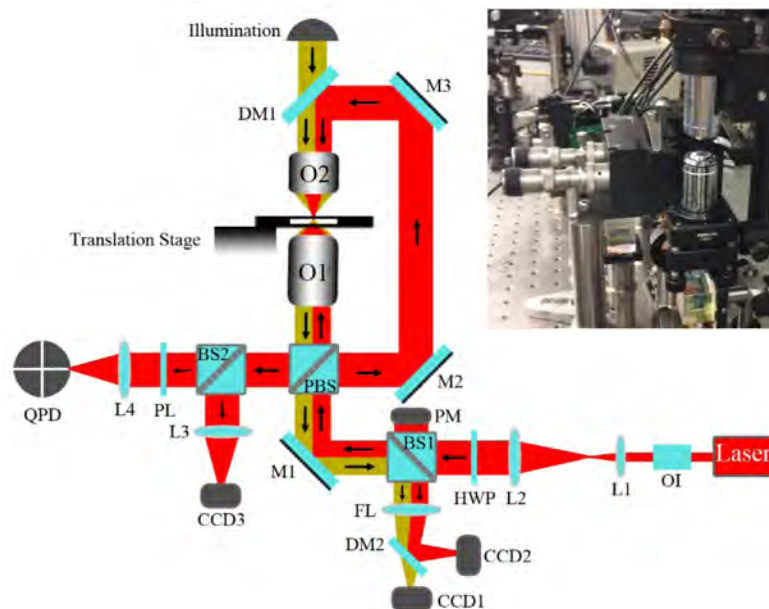

Fig. 4. Layout of the optical trapping system. OI: optical isolator; L: lens; HWP: half waveplate; M: mirror; BS: beam splitter; PBS: polarizing beam splitter; DM: dichroic mirror; O: objective lens; FL: field lens; PL: polarizer; QPD: quadrant photodiode; PM: power meter; CCD: charge coupled device. Inset shows part of the system.

Figure 4 shows the layout of the convertible optical trapping system, which includes the following four modules:

- **Trapping module**: A near infrared laser with a wavelength of 1064 nm is used as the trapping laser. The laser passes through an optical isolator (OI) to avoid back reflection. It is then expanded and collimated with two lenses (L1 and L2) in the form of a telescope to overfill the back aperture of the objective lenses (O1 and O2). A half-wave plate (HWP) and a polarizing beam splitter (PBS) are combined to split the beam into two cross-polarized beams. The relative power in each beam can be adjusted by rotating the HWP. Mirrors M1, M2, M3 and the dichroic mirror DM1 help to guide the beams to the two objective lenses O1 and O2. The two CP beams with cross polarizations are then focused into the sample chamber. O2 is mounted on a piezo stage for precise alignment of the two beams. The two objective lenses are configured perpendicular to the optical table for mechanical stability. The sample chamber containing the particles is mounted on a 3D translation stage. A detailed instruction for the preparation of the sample chamber will be given in section 4.5. The two trapping modes - SB or CP trap - can be switched easily by rotating the HWP while keeping the whole system unchanged. For example, the system can be converted to a SB trap if the HWP is rotated to a position where all the light transmit through O1.

- **Imaging module**: This module is used for the real-time imaging of the particles. A white light is coupled to the trapping module through DM1 and then focused on the sample by O1 for illumination. The particles can be imaged on CCD1 by O1 and a field lens (FL).

- **Detecting module**: This module is used to track the real-time position of the particles based on the forward scattering method [39–45]. The two CP beams passing through the rectangular ring formed by PBS, M2, M3 and DM1 will eventually come out of the forth facet of the PBS. One beam passes the ring clockwise, the other counter-clockwise. This is similar to the light path in a Sagnac interferometer except that there is no interference because of the cross polarization of the two beams. Either of the beam can be picked by a polarizer (PL) for the position tracking.

- **Alignment module**: This module is indispensable for the successful realization of the convertible optical trapping system because the alignment is critically important. For example, the foci of the two CP beams must be well overlapped both transversely and longitudinally to form a stable CP trap. Briefly, the two CP beams that pass through the forth facet of the PBS are reflected by BS2 and focused on CCD3 by lens L3. The light spots showing on CCD3 can be used to check the real-time alignment of the two foci. In addition, it is also necessary to find the sample surface in the experiment, which can be achieved by imaging the reflected light from the sample surface on CCD2 with O1 and FL. Finally, it is also important to know the laser power at the trapping position, which can be calibrated by knowing the laser power at the BS1 and the rotation angle of the HWP.

Here are some other considerations that one should take into account:

- **Laser:** the choice of the laser wavelength depends on the applications. For bio-related applications, near-infrared lasers are commonly used because of the low absorption on bio-materials in this spectrum. Another important factor that must be taken into account is the vibration isolation of the laser. This can be done by the following two ways:

(1) Isolate the vibration from the laser with an optical fiber as schematically shown in Fig. 5(a). Single-mode and polarization-maintaining (PM) fiber is typically used to

maintain a good Gaussian profile of the laser as well as the polarization. This method can well isolate the vibration from the laser system, but requires tedious light-fiber coupling if the laser itself is not fiber coupled. In addition, small vibration of the optical fiber will cause detectable fluctuations of the laser power, especially when polarization optics are used in the system. Therefore, this configuration is not recommended for the convertible optical trapping system since PBS is used;

(2) Choose laser head without fans and put it on the same optical table where the trapping system locates as schematically shown in Fig. 5(b). This configuration does not require the time-consuming light-fiber coupling, but the laser head should have minimum vibration. Therefore, laser with watering cooling option is recommended. We use an infrared laser from Laser Quantum (Ventus 1064, 5W) together with a water cooling system (Oasis 170). The laser head and the trapping system are on the same optical table, but the power supply units for the laser and the cooling system are isolated from the optical table.
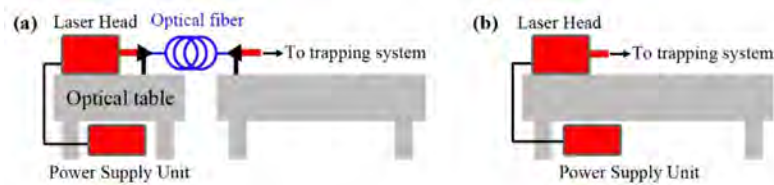

Fig. 5. (a). Isolate the laser vibration with an optical fiber. (b) Choose a laser with minimum vibration in the laser head.

• **Objective lens:** the proper choice of the objective lens in terms of aberration, transmission, and NA is another important factor that must be carefully taken into account both for the trapping and imaging.

(1). **Aberration:** It should be noted that most off-the-shelf commercial objective lenses for optical microscopes (Nikon, Olympus, Leica, Zeiss) are designed and optimized in the visible spectrum. Therefore, they still suffer from spherical aberration for the infrared lasers that are commonly used in the trapping system. The spherical aberration must be carefully taken into account in a SB trap, which introduces an important dependence on the trapping height above the coverslip [18,46]. In contrast, the negative effect of the spherical aberration in a CP trap is alleviated due to the cancellation of the scattering forces.

(2). **Transmission:** Most objective lenses have low transmission in the infrared spectrum. For example, we have measured the transmission of Nikon's objective lens (CFI Plan Apochromat VC Series 100x/1.4NA oil immersion) and found a 30% transmission at the wavelength of 1064 nm. The low transmission of the objective lens means high laser power at the entrance of the objective lens, which may rise the temperature of the system and result in system drift that must be avoided for sensitive force measurement. Nikon has introduced the high performance objective lenses with nano-crystal coat technology (CFI60 Plan Apochromat Lambda Series) and claimed dramatically increase in the transmission across a broad spectrum range, which may be a good option to increase the transmission for the trapping laser. In our system, two low-cost objective lenses O1 (AmScope, NA = 1.25, 100x, Oil) and O2 (AmScope, NA = 0.65, 40x, Air) with a measured transmission of 45% and 68%, respectively, are used.

(3). **Numerical aperture (NA)**: In SB trap, the objective lens typically has a large NA, therefore, oil or water-immersion objective lenses are commonly used. Water-immersion objective lenses can minimize the spherical aberrations that originate

from the refractive-index mismatch between water and glass, which is important for trapping particles far away from the surface. However, water-immersion objective lenses are more expensive than oil-immersion objectives. Therefore, oil-immersion objective lenses are good choice for a tight budget. It should be noted that an oil-immersion objective lens with a larger NA does not necessary result in better trapping. This is mainly because the effective NA of an oil-immersion objective lens is limited by the total internal reflection from the water-glass surface, which will not exceed 1.3 for trapping in water solution. Based on these facts, a low-cost oil-immersion objective lens from AmScope is used (NA = 1.25, 100x, Oil) in the convertible optical trapping system.

4. Details on the realization of the convertible optical trapping system

The well alignment of the two foci from the CP beams is critically important for the successful realization of the convertible trapping system. In addition, the well overlap of the objective plane of O1 with the trapping plane is important to the imaging. Therefore, the alignment details for these two situations are given in this section. The alignment of other optical elements, such as the lenses, mirrors, beam splitters, and QPD, to the optical axis has been well documented in [10,47], therefore, we simply assume that these optical elements have been well aligned to the optical axis.

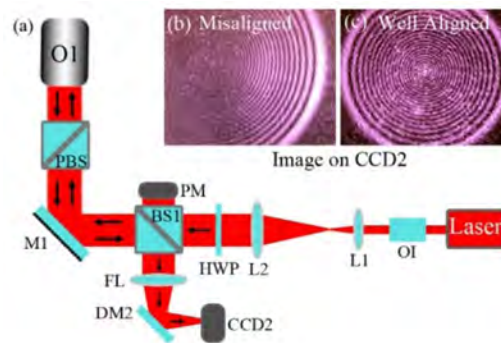### 4.1 Align the objective lenses to the optical axis

Fig. 6. (a) Align objective O1 to the optical axis with the reflected light from the back aperture of O1. (b) The image on CCD2 shows the objective lens is misaligned. (c) The image on CCD2 shows the objective lens is well aligned to the optical axis.

To construct the convertible optical trapping system, the centers of the two objective lenses O1 and O2 must be well aligned to the optical axis. For this purpose, the objective lenses O1 and O2 are mounted on two 5-axis locking kinematic mount (Thorlabs, K5X1) for five degrees of freedom of adjustments. Adapters with external SM1 threads and internal RMS threads (Thorlabs, SM1A3) are also needed to correctly fit the objective lenses to the mounts. The reflected light from the back aperture of O1 is imaged on CCD2 to check the alignment as shown in Fig. 6(a). Figure 6(b) shows the reflected light pattern on CCD2 when O1 is misaligned from the optical axis. Figure 6(c) shows the light pattern when O1 is well aligned to the optical axis by adjusting the 5-axis kinematic mount. One can follow the same procedure to align the second objective lens O2 to the optical axis.

4.2 Overlap the objective plane to the trapping plane

Most objective lenses that are designed for optical microscope are infinity-corrected, which means the image plane of the objective lens (conjugate to the objective plane) is at infinity. Therefore, a field lens (FL) is required to bring the image back on a CCD. The advantage of using an infinity-corrected objective lens lies in the freedom of adding other optical elements

in the system with minimum perturbation of the optical path. Since the objective lens O1 is used for both imaging and trapping, it is important to make sure the objective plane overlaps with the trapping plane. The objective plane of an infinity-corrected objective lens is located near the focus for the best image quality as shown in Fig. 7. The objective plane can be found by placing a marker, such as a US air force target (Thorlabs, R3L3S1P), on a translation stage under visible light illumination. Move the target near the focus of O1 along the optical axis till a clear image of the target with the best quality is formed on CCD1. Since the trapped particle will also have the best image quality at this objective plane, it is necessary to overlap the trapping plane with the objective plane. However, these two planes do not overlap automatically because of the spherical aberration of the system and the divergence of the trapping laser. To make these two planes overlap, one can follow the procedures below:
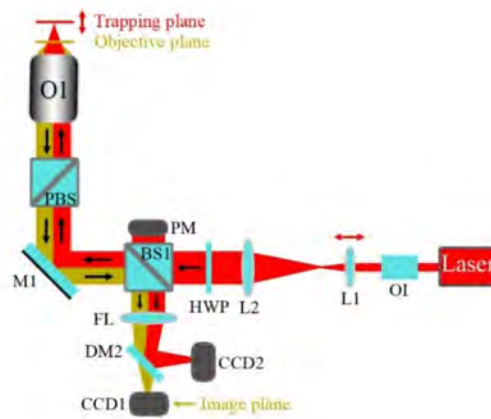

Fig. 7. Procedures to overlap the objective plane of O1 to the trapping plane.

(1) Once the objective plane of O1 is found in the previous step, keep the target at this position;

(2) Move CCD2 till a clear image of the target is formed on CCD2 under the trapping laser illumination. The trapping laser spot on the target should also appear on CCD2 at this step;

(3) Gently move lens L1 along the optical axis while keeping your eyes on CCD2 till the laser spot is minimum on the target. Now the trapping plane overlaps with the objective plane.

The image on CCD2 can also be used to determine the sample surface, which is useful to get information such as the trapping height of the particle above the surface. At the start of the experiment, the sample containing the particles can be moved along the optical axis till a minimum spot from the reflected light on the sample surface is formed on CCD2. At this step, the trapping laser is exactly focused on the sample surface. One can also double check the image on CCD1, which should give a clear image of the defects on the surface if there is any.

4.3 Overlap the foci of the two CP beams

Align the two objective lenses to the optical axis as described in section 4.1 does not guarantee the foci overlap of the two objective lenses, but one should see two spots on CCD3 as shown in Fig. 8(a). These two spots come from the two CP beams that transmit through the forth facet of the PBS. The sizes of the two spots are different because the different NA of the two objective lenses. If two identical objective lenses are used in the system, one should see two identical spots. The two foci of O1 and O2 will overlap transversely in the trapping plane if these two spots overlap on CCD3. This can be achieved by moving O2 transversely and

adjusting mirror DM1 as shown in Fig. 8(c). In our system, O2 is mounted on a piezo objective actuator (EO Edmund, Stock No. 85-008) for vertical displacement. The piezo objective actuator is then mounted on a 5-axis locking kinematic mount (Thorlabs, K5X1) for lateral displacement. Figure 8(b) shows that the two foci are well aligned. However, the overlap of the two foci in the transverse direction does not guarantee their overlap along the optical axis. The overlap along the optical axis can be checked by scanning a GNP through the two foci as follows:
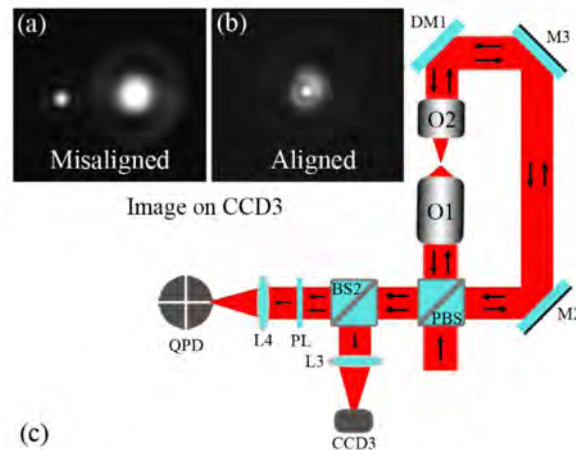

Fig. 8. Procedures to overlap the foci of the two CP beams focused by O1 and O2.

(1). Put one droplet of solution containing 200nm GNPs on a glass coverslip;

(2). Let the solution evaporate, the GNPs will stick on the glass surface;

(3). Put one droplet of immersion oil on the GNPs to match the reflective index of glass;

(4). Cover the GNPs and the immersion oil with another glass coverslip;

(5). Insert this GNP sample between O1 and O2 on a piezo-stage;

(6). Block the beam from O2 and position one GNP at the focus of O1 by looking at the back-scattering light from the GNP on CCD2 (Fig. 7);

(7). Block the beam from O1, one should see the back-scattering light of the same GNP from O2 also appears on CCD2; If the GNP is not at the focus, adjust DM1 to make it at the center (DO NOT move the GNP at this step);

(8). Scan the GNP transversely across the focus of O2 while keeping your eyes on the image of CCD2.

(9). Move O2 along the optical axis with the piezo objective actuator and repeat step (8) till one can tell that the GNP passes the beam waist of the laser focused by O2.

After doing all these steps, the two foci of the CP beams overlap both transversely and longitudinally. Now, one can save the image of the light spots on CCD3 for future reference. For example, one do not need to repeat this alignment procedure in every experiment, just move O2 along the optical axis till the light spots on CCD3 are similar to the one on record. This trick turns out work very well in the experiment and save the time to realign the system in every experiment.

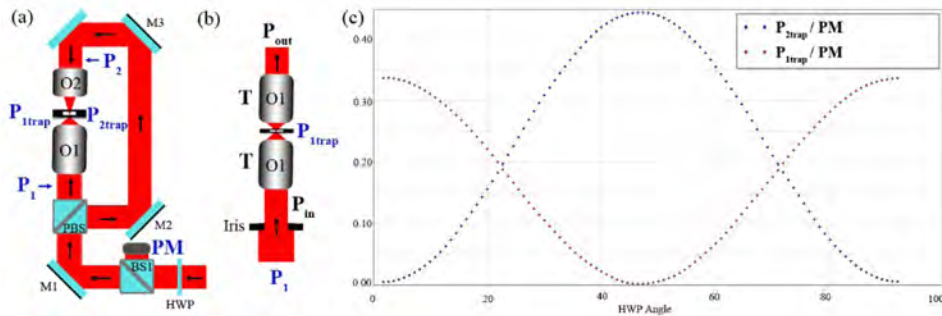## 4.4 Calibrate the trapping power

Fig. 9. Procedures to calibrate the laser power at the trapping position. (a) Laser power check points. (b) Measure the laser transmission of the objective lens. (c) The calibrated curve for the laser power at the trapping position.

In the convertible optical trapping system, the laser powers of the two CP beams at the trapping position must be carefully calibrated. This can be done by monitoring the laser power at BS1 with a power meter and recording the rotation angle of the HWP as shown in Fig. 9(a). The laser powers of the two CP beams at the trapping position can be calibrated as follows:

(1) Record the power at PM, P1, and P_2 as a function of the HWP angle as shown in Fig. 9(a);

(2) Calculate the power ratio P_1/PM and P_2/PM as a function of the HWP angle.

(3) The power transmission P_{1trap}/P_1 and P_{2trap}/P_2 can be measured according to Fig. 9(b) (described below), where P_{1trap} and P_{2trap} is the laser power of the two CP beams at the trapping position, respectively.

(4) Calculate the final power ratio P_{1trap}/PM and P_{2trap}/PM as a function of the HWP angle according to the following equations: $P_{1trap}/PM = (P_{1trap}/P_1)(P_1/PM)$ and $P_{2trap}/PM = (P_{2trap}/P_2)(P_2/PM)$.

Figure 8(c) shows the calibrated laser power for the two CP beams. In the experiment, the laser powers at the trapping position for the two CP beams can be immediately found from these two curves if the power (PM) at BS1 and the HWP angle are known.

The power transmission P_{1trap}/P_1 can be measured according to Fig. 9(b) as follows: (same for P_{2trap}/P_2)

(1) Replace O2 in Fig. 9(a) with an identical objective lens O1 and put a variable Iris before O1 as shown in Fig. 9(b).

(2) Align the two CP beams according to the procedure described in section 4.3.

(3) Slowly close the Iris while monitoring the output power P_{out} till P_{out} starts to change.

(4) Record P_{out}, P_{in}, and P_1 as shown in Fig. 9(b).

(5) The transmission due to truncation of the beam from the back aperture of O1 is P_{in}/P_1, the transmission due to the objective lens O1 and the sample chamber is $\sqrt{(P_{out}/P_{in})}$.

Therefore, $P_{1trap}/P_1 = (P_{in}/P_1) \sqrt{(P_{out}/P_{in})}$.

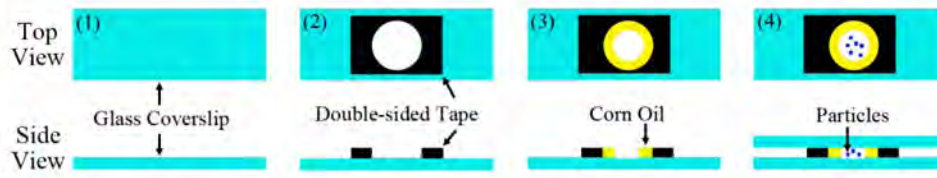### 4.5 Prepare a well-sealed sample chamber

Fig. 10. Procedures to prepare a well-sealed sample chamber.

In this section, a quick and simple way to prepare a well-sealed sample chamber is described. Figure 10 schematically shows the procedures as follows:

(1) Place a clean glass coverslip (0.16 – 0.19 mm) on a flat surface such as a glass slide.

(2) Punch a hole on a double-sided tape with a ticket punch and stick the tape on the glass coverslip. The hole on the double-sided tape forms the chamber that will hold the particle solution.

(3) Use a pipette to spread some corn oil (or any cooking oil that one can get from grocery store) around the inner perimeter of the hole (see step 3 in Fig. 10). This ring-shaped oil will prevent the particle solution from evaporation.

(4) Add one droplet of particle solution at the center of the ring-shaped oil and place another glass coverslip on top.

(5) Push tight the two glass coverslips.

A well-sealed sample chamber can be formed if one follows these steps. The chamber prepared in this way can be used for the trapping within one week without obvious solution leakage and evaporation.

5. Results and discussion

In SB trap, the trapping position locates above the beam center due to the scattering force as shown in Fig. 2(a), which results in a reduced trapping strength in the transverse direction compared to that trapped at the beam center. The trapping position for a given particle cannot be changed easily in a SB trap. In contrast, the trapping position can be adjusted in a CP trap by either changing the relative power of the two beams or moving objective lens O2 as schematically shown in Fig. 11(a).
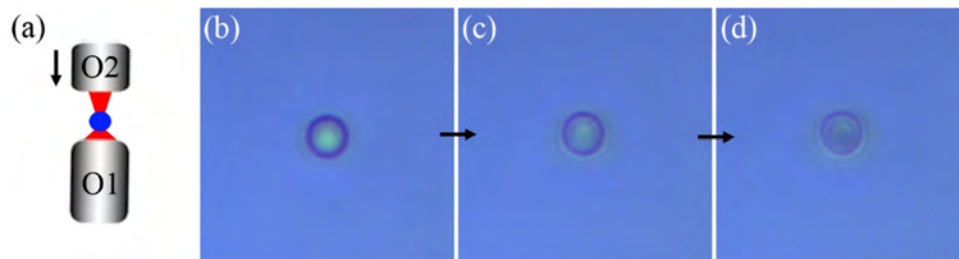

Fig. 11. (a) Change the trapping position of a polymer bead along the optical axis by moving the objective lens O2. (b) – (d) sequential images of the polymer bead when moving O2 downward (see Visualization 1).

Figure 11(b) shows the image (on CCD1) of a polymer bead with a diameter of 2.1 µm that is trapped with the convertible optical trapping system. The polymer bead is trapped at the objective plane of O1 so that the bead is clearly imaged on CCD1 (trapping position overlaps with the objective plane as discussed in section 4.2). Figure 11(c) and 11(d) shows

the image of the same trapped polymer bead when moving O2 downward. The polymer bead is pushed below the objective plane and out of focus of O1 (see Visualization 1). Therefore, the trapping position in a CP trap can be tuned flexibly along the optical axis, which provides another freedom to optimize the trapping strength of the particle.
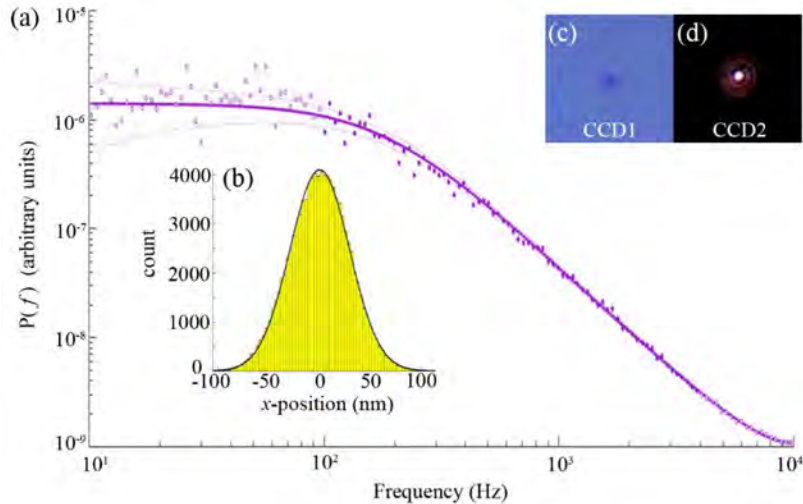

Fig. 12. (a) Power spectra of a 200 nm GNP in a CP trap (dot points). Full line shows the fit using the method described in [48]. Dashed lines show the standard deviation of the blocked data points according to which are Gaussian distributed around their expectation value (full line). (b) Position distribution of the 200 nm GNP along the transverse direction (x direction) in the CP trap. (c) and (d) shows the image of the GNP trapped in the CP trap on CCD1 and CCD2 (Fig. 4), respectively. (see Visualization 2 and Visualization 3).

To further demonstrate the advantage and robustness of this convertible optical trapping system, GNP with diameter of 200 nm is also trapped on this system. Figure 12(a) shows the power spectra of a 200nm GNP in the CP trap in the transverse direction, which is perpendicular to the optical axis. The data analysis are performed with a Matlab package as described in [48], which has been widely used for data analysis in the optical trapping community [19–21]. Full line shows the fit using the method described in [48]. Dashed lines show the standard deviation of the blocked data points according to which are Gaussian distributed around their expectation value (full line). The trapping power at the trapping positon is P_{1trap} = 3.3 mW and P_{2trap} = 9.3 mW, respectively, for the two CP beams as shown in Fig. 9(a). The optical trapping strength can be determined by the trap stiffness κ_x, which is measured to be κ_x = (0.15 ± 0.01) pN/(nm·W) normalized to the laser power. The GNP is trapped 5 μm above the sample surface to avoid the proximity effects. Figure 12(b) shows the position distribution of the GNP in the CP trap, which follows a Gaussian distribution assuming a linear relationship between the position and the QPD signal.

It should be noted that the 200nm GNP cannot be trapped with the SB trap on this system, which verifies the benefit of trapping highly scattering particles with CP trap. This also agrees with our theoretical calculations shown in Fig. 2(b). Figure 12(c) and 12(d) shows the image of the 200nm GNP in the CP trap on CCD1 and CCD2 (see Visualization 2 and Visualization 3), respectively. The image of the trapped GNP from the transmitted light is shown on CCD1, while the image of the trapped GNP from the back-scattering light is shown on CCD2. GNP of this size has been reported trapped successfully in a SB trap [19]. The discrepancy is attributed as follows: (1) Spherical GNPs are assumed in the theoretical calculation. However, the GNPs used in the experiment vary in shape and size, which influences the trapping ability significantly. This has been also observed by Oto et al. [49,50]; (2) The truncation of the beam by the objective lens is not taken into account in the calculation, which can also alter

the trapping ability [51,52]; (3) The spherical aberration of the objective lens in [19] is carefully minimized, while it is not taken care of in our system. Besides, the same group later shows that the 200 nm GNPs are actually not trapped on the optical axis [18], which means that the trap strongly depends on the experimental conditions. Therefore, it is important to compare the trapping ability under the same experimental conditions. The convertible optical trapping system introduced in this article provides an ideal platform for this purpose.

We expect the readers with basic knowledge in optics can replicate or re-model this system for their own research. The system can also be easily converted into a dual-beam trapping system if the foci of the two CP beams are offset rather than overlapped. Therefore, this convertible optical trapping system not only maintains the trapping capability of the state-of-the-art optical tweezers, but also allows for the trapping of a wide variety of particles that a conventional optical tweezer cannot handle.

Acknowledgments